

Analysis of Doppler-broadened Bi $K\alpha$ x-ray lines observed in 460-MeV Xe + Bi collisions

R. Anholt*

Department of Physics, Stanford University, Stanford, California 94305

(Received 17 June 1977)

The Bi $K\alpha$ lines observed in 460-MeV (lab) Xe + Bi encounters are significantly Doppler broadened. The x-ray line shapes can be calculated using theoretical models for the impact-parameter dependence $P(b)$ of the probability of making $1s\sigma$ vacancies in Xe + Bi collisions. The measured line shapes are in good agreement with those derived from values of $P(b)$ calculated by Betz *et al.*

I. INTRODUCTION

Recently there has been much speculation about the impact-parameter dependence $P(b)$ of the probability of making $1s\sigma$ vacancies in 1600-MeV $U+U$ collisions.¹⁻⁵ The magnitude of $P(0)$ indicates whether it is possible to observe spontaneous or induced positron decay when the $1s\sigma$ level dives into the negative energy sea.^{4,6} Generalizing from collisions with atomic numbers $Z \leq 50$, where the binding effect is important,^{2,3,5} predicted $P(0)$ values for $U+U$ collisions are of the order of 10^{-5} to 10^{-4} .^{2,3} Recently, however, Betz *et al.*⁴ made approximate perturbed-stationary-states calculations of $P(b)$ using relativistic wave functions and obtained $P(0)=0.045$. The difference between the prior extrapolations and the new predictions can be understood qualitatively by introducing correction factors for electronic relativistic effects.⁵

To test the predictions of Betz *et al.*,⁴ the cross section and $P(b)$ must be measured in asymmetric collisions where the K x rays emitted by the higher- Z collision partner result solely from excitation of electrons from the $1s\sigma$ molecular orbital (MO).⁵ Most K x rays observed in nearly symmetric collisions result from the excitation of electrons from the $2p\sigma$ MO.^{2,7} [$P(b)$ shall denote $P_{1s\sigma}(b)$ in this paper.] An ideal projectile-target combination for measuring $P(b)$ and $\sigma_{1s\sigma}$ is ${}_{54}\text{Xe}^{136} + {}_{83}\text{Bi}^{209}$. In these collisions, the Bi K x rays signal $1s\sigma$ -vacancy formation. Also, the Bi K -vacancy production cross section has a negligible contribution from nuclear Coulomb excitation followed by internal conversion.⁷

Predictions of $P(b)$ may be tested by measuring the Doppler-broadened line shape of the Bi K x rays. Doppler broadening of the target K x rays requires (i) that most of the $1s\sigma$ vacancies should be made in collisions with small impact parameters where the target atom receives the largest possible energy transfer from the projectile and (ii) that the ratio of the projectile to target mass should be sufficiently large so that the target

atom receives a large energy transfer. The first requirement is most important. In most K x-ray measurements with target atoms with $Z \leq 50$ and comparable masses of the projectile and target, Doppler broadening of the target K x rays is small compared with the resolution of solid-state detectors. In those encounters most $1s\sigma$ and $2p\sigma$ vacancies are made in collisions with large impact parameters where the target atom remains nearly stationary.

While this work was in progress Greenberg *et al.*⁸ independently proposed a method for measuring $P(b)$ based on the fact that $P(b)$ can be uniquely extracted from measurements of line shapes of x rays detected at 0° with respect to the beam. Also, by using the Kessel model¹⁰ for $P(b)$ [$P(b) = P(0)$ for $b \leq b_0$ and $P(b) = 0$ for $b > b_0$], Behncke *et al.*⁹ were able to extract critical impact parameters b_0 from measurements of linewidths of K x-ray lines observed at 90° with respect to the beam.

II. METHOD

Line shapes were measured at the Berkeley SuperHILAC using a 460-MeV Xe^{136} beam and a 1-mg/cm² Bi^{209} target. An intrinsic Ge planar x-ray detector with a resolution of 480 eV for the Bi $K\alpha$ lines was used to detect the Bi K x rays. The 74- and 77-keV Bi $K\alpha$ lines were observed at 6 angles between 10° and 130° . The detector subtended an angle of 6° . No attempt was made to analyze the Bi $K\beta$ lines because of their complex structure.

To calculate x-ray line shapes, the double differential cross section¹¹ for the inelastic scattering of the projectile into a center of mass (c.m.) solid angle $d\Omega_1$ and the emission of an x ray into a CM solid angle $d\Omega_x$ must be considered:

$$\frac{d\sigma(\Theta_1, \Phi_1, \theta_x, \phi_x)}{d\Omega_1 d\Omega_x} = \frac{d\sigma_R p(\Theta_1)}{d\Omega_1 4\pi}. \quad (1)$$

Here $d\sigma_R/d\Omega_1$ is the Rutherford-scattering cross section, $p(\Theta_1) = \alpha P$ [$b = (d_0/2) \cot(\Theta_1/2)$], d_0 is the distance of closest approach in head-on encounter-

ers, and α is the probability that the Bi K vacancy will decay emitting a $K\alpha_1$ or $K\alpha_2$ x ray. We assumed that the K x rays are emitted isotropically in the c.m. system. [We found that the Bi $K\alpha$ x rays are emitted isotropically to within 3% in the laboratory (lab) system.] The relationship between the energy of the Doppler-shifted x ray E_x and the unshifted energy E_{x0} is given by

$$E_x = E_{x0}(1 - \beta^2)^{1/2} / (1 - \beta \cos \theta_{x2})$$

$$\approx E_{x0}(1 - \frac{1}{2}\beta^2) / (1 - \beta \cos \theta_{x2}), \quad (2)$$

where $\beta = v_2/c$, v_2 is the lab velocity of the recoiled target atom, and θ_{x2} is the angle between \vec{v}_2 and the direction of the emitted photon. The use of Eqs. (1) and (2) to calculate the cross section for the emission of photons $d^2\sigma/dE_x d\Omega'_x$ into a lab solid angle $d\Omega'_x = d \cos \theta'_x d\phi'_x$ with energy E_x is described in Ref. 11. The relationship between θ_{x2} and v_2 and the angles θ'_x , ϕ'_x , Φ_1 , and Θ_1 may be used to solve for $\cos \Theta_1$ as a function of E_x , Φ_1 , ϕ'_x , and θ'_x . The cross section can then be written

$$\frac{d\sigma(E_x, \theta'_x, \phi'_x)}{dE_x d\Omega'_x} = \frac{d\Omega_x}{d\Omega'_x} \int d\Phi_1 \frac{d \cos \Theta_1}{dE_x} \frac{d\sigma_R p(\Theta_1)}{d\Omega_1 4\pi}. \quad (3)$$

Since Θ_1 depends on E_x as well as Φ_1 , to obtain the Doppler-broadened line shapes at $\theta'_x \neq 0^\circ$, we must integrate over $p(\Theta_1(\Phi_1))$. (For further details, see Ref. 11.)

Two additional integrations must be made.¹¹ First, one must integrate over the detector solid angle $d\Omega'_x$. This integration affects the line shape insignificantly; hence, the line shape at the angle θ'_x between the center of the detector and the beam direction was calculated, and the distribution was multiplied by a constant solid angle $\Delta\Omega'_x$. Second, an integration over the finite target thickness should be made. Since the energy loss by the projectile is negligible with respect to the beam energy, we approximated this integration by multiplying the cross section for the initial beam energy by the target thickness.

Finally, we must account for two other sources of broadening of the Bi $K\alpha$ lines: the detector resolution and unresolved satellite-peak structure. The detector resolution is easily accounted for by folding a 480-eV full width at half maximum (FWHM) Gaussian detector response function into the calculated Doppler line shape. The detector response was measured using radioactive sources.

Unresolved satellite-peak broadening can only be estimated. Satellite peaks arise because of the presence of outer shell vacancies when the K x ray is emitted. A shift in the Bi $K\alpha$ line of 137 eV for every L vacancy present can be expected.¹² We neglect smaller shifts due to the presence of M and N vacancies. Since the detector

resolution is 480 eV, it is not possible to resolve individual peaks. However, one can measure the average line shift. Behncke *et al.*⁹ measured shifts of 280 eV in 4.66-MeV/amu Pb+ Z_2 collisions with $Z_2 > 40$. This indicates the presence of about two Pb L vacancies on the average from which we can expect a distribution of 0 to 4 L vacancies. Assuming that the distribution is approximately Gaussian, we therefore expect that the un-Doppler-broadened Bi $K\alpha_1$ and $K\alpha_2$ lines are Gaussian with widths of about 550 eV. The satellite peak width may be less in 3.5-MeV/amu Xe+Bi encounters because of the lower projectile velocity. Also, multiple-collision L -shell stripping may increase the number of Pb L vacancies when Pb is the projectile.

The detector resolution and satellite-peak broadening can be taken into account by folding into the calculated Doppler line shape a Gaussian response function with a FWHM Δ_x given by

$$\Delta_x = (\Delta_d^2 + \Delta_s^2)^{1/2} = 730 \text{ eV}, \quad (4)$$

where $\Delta_d = 480$ eV is the detector resolution and $\Delta_s = 550$ eV is the satellite linewidth. Figure 1 compares calculated line shapes observed at 90° and 10° using Gaussian response functions with widths of 430 eV ($= \Delta_d$, the detector resolution only) and 730 eV ($= \Delta_x$, the detector resolution plus estimated satellite-peak broadening). The $P(b)$ values calculated by Soff using Betz's method⁴ were used in this comparison. Near the $K\alpha_1$ and $K\alpha_2$ peaks the distribution calculated using the smaller detector resolution width Δ_x is sharper. However, at the wings of the lines where the Dop-

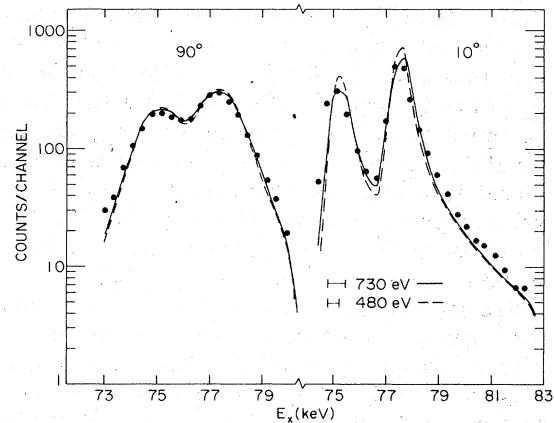


FIG. 1. Comparison of measured (points) and derived (curves) photon distributions observed at 90° and 10° . The derived distributions were calculated using detector response functions with widths of 480 eV (the detector resolution) and 730 eV (detector resolution plus estimated satellite-peak broadening). Soff's calculated $P(b)$ values were used (Ref. 4).

pler line shape depends less steeply on E_x , the calculations using the two different linewidths are nearly identical. Therefore, as long as the comparison between the calculated line shapes and experiment is done at the wings of the line instead of near the $K\alpha_1$ and $K\alpha_2$ peaks, the comparison will be relatively insensitive to the uncertainty in the satellite linewidth. A response function with a 730-eV FWHM is used throughout the remainder of this paper.

III. RESULTS

Figure 2 compares experimental and calculated photon distributions observed at six angles between 10° and 130° . In this figure, the $P(b)$ values calculated by Soff using Betz's method were used. The agreement between the calculated and observed distributions is good indicating that Soff's calculation of the shape of $P(b)$ in Xe+Bi encounters is fairly accurate. However, the absolute magnitude of $P(b)$ is not used in these comparisons since the experimental and calculated distributions are normalized to the same area under the $K\alpha$ line. The absolute magnitude of the theoretical $P(b)$ is easily tested by comparing 1σ -vacancy production cross sections. For 460-MeV Soff calculated $\sigma_{1\sigma} = 1.1$ b whereas we observed 2.1 b.

In obtaining the experimental photon distribution shown in Fig. 2, a continuum background with approximately 300 counts/channel on the low-energy side of the $K\alpha$ peak and 100 counts/channel on the high-energy side was subtracted. The shape

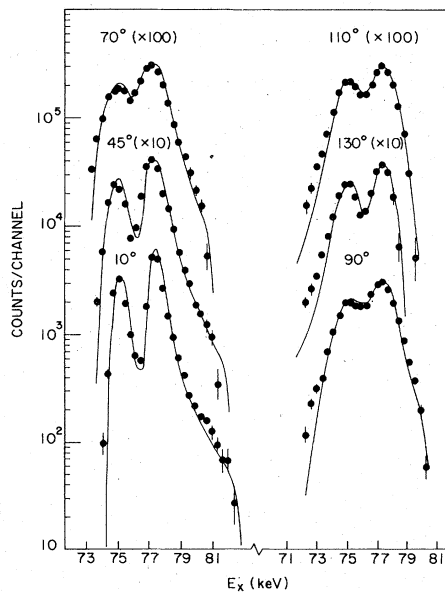


FIG. 2. Experimental and theoretical distributions observed at 10° , 45° , 70° , 90° , 110° , and 130° .

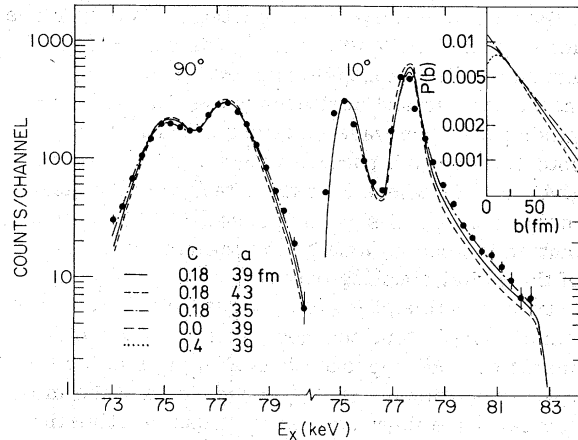


FIG. 3. Experimental and theoretical photon distributions observed at 10° and 90° calculated using Eq. (5) and various values of the falloff parameter a and the constant C which determines $P(0)$. (The values of A and d are held constant. The dotted and long-dashed curves cannot be distinguished from the solid curve.)

and magnitude of this background is uncertain, hence the minor deviations between theory and experiment at the far wings of the lines are not significant.

Additional evaluations of the Doppler-broadened line shapes were made to see how sensitive the line shapes are to the detailed form of $P(b)$. Soff's results can be written

$$P(b) = A \exp(-b/a) [1 - C \exp(-b/d)], \quad (5)$$

where $A = 0.011$, $a = 39$ fm, $C = 0.18$, and $d = 5.25$ fm. Figure 3 shows calculations using different values of a and C . While the line shape is very sensitive to the value of the fall-off parameter a , it is not sensitive to the constant C which, when A , a , and d are held constant, determines the magnitude of $P(0)$. Furthermore, one can conclude from Fig. 3 that a falloff parameter of $a = 35$ fm fits the distributions better than $a = 39$ fm computed by Soff.

IV. CONCLUSIONS

Betz's calculations of the probability for making 1σ vacancies $P(b)$ predict the shape of the Doppler-broadened Bi $K\alpha$ x rays observed in 460-MeV Xe + Bi collisions fairly accurately. The cross section calculated by Betz *et al.*⁴ is a factor of only 0.5 lower than experiment. Since prior predictions^{2,3} for 1600-MeV $U+U$ collisions and similar predictions for Xe+Bi encounters give $P(0) = 10^{-4}$ to 10^{-5} , the present work is an important experimental verification of Betz's results for Xe+Bi collisions.

Betz's calculations are expected to be even more accurate in $U+U$ collisions.¹³ The calculations are based on a monopole approximation to the molecular $1s\sigma$ and continuum wave functions. Atomic electron wave functions calculated for a potential due to a nucleus with a blown-up radius given by $\frac{1}{2}R$, where R is the internuclear distance in the actual collision, are used.^{4,13} This approximation is good as long as the matrix elements of the radial coupling operator $\partial/\partial R$ have their maximum value at $R=0$.¹³ In quasimolecules with small united atom charges Z_{UA} the matrix elements of $\partial/\partial R$ approach 0 as R approaches 0 for $\sigma \rightarrow \sigma$ transitions. As Z_{UA} decreases and the molecular wave functions become less relativistic than in $U+U$ quasimolecules, and become less dominated by the finite nuclear potential, the

monopole approximation will be less good. For Xe+Bi, Z_{UA} is equal to 137. This is approximately the lowest value of Z_{UA} where the monopole approximation remains valid.¹³ Nevertheless, we have shown that the calculated $1s\sigma$ cross section agrees within a factor of two with experiment, even at this low value of Z_{UA} , and that the calculated $P(b)$ values accurately predict the shape of the Doppler-broadened Bi $K\alpha$ rays.

ACKNOWLEDGMENTS

The author wishes to thank W. E. Meyerhof, I.-Y. Lee, and Y. El Masri for supporting and encouraging these experiments and G. Soff for providing calculations of $P(b)$ for 460-MeV Xe + Bi encounters. This work was supported in part by the NSF.

*Present address: Gesellschaft für Schwerionenforschung, P. O. Box 110541, 6100 Darmstadt 1, W. Germany.

¹D. Burch, W. B. Ingalls, H. Wieman, and R. Vandebosch, *Phys. Rev. A* **10**, 1254 (1974).

²C. Foster, T. Hoogkamer, P. Woerlee, and F. W. Saris, *J. Phys. B* **9**, 1943 (1976).

³W. E. Meyerhof and R. Anholt, in *Abstracts, Second International Conference on Inner Shell Ionization Phenomena*, edited by W. Mehlhorn (University of Freiburg, Germany, 1976), p. 56.

⁴W. Betz, G. Soff, B. Müller, and W. Greiner, *Phys. Rev. Lett.* **37**, 1046 (1976); W. Betz, G. Heiligenthal, B. Müller, V. Oberacker, J. Reinhardt, W. Schäfer, G. Soff, and W. Greiner, invited talk at the International Summer School on Nuclear Physics, Predeal, Rumania, 1976 (unpublished). The Xe+Bi calculations were made by G. Soff.

⁵R. Anholt and W. E. Meyerhof, *Phys. Rev. A* **16**, 190 (1977).

⁶K. Smith, H. Peitz, B. Müller, and W. Greiner, *Phys. Rev. Lett.* **32**, 554 (1972).

⁷W. E. Meyerhof, R. Anholt, T. K. Saylor, S. M. Lazurus, and L. F. Chase, Jr., *Phys. Rev. A* **14**, 1653 (1976).

us, and L. F. Chase, Jr., *Phys. Rev. A* **14**, 1653 (1976).

⁸J. S. Greenberg, H. Bokemeyer, H. Emling, E. Grosse, D. Schwalm, and H. J. Wollersheim, *Abstracts of the Tenth International Conference on the Physics of Electronic and Atomic Collisions, Paris, 1977*, edited by M. Barat and J. Reinhardt (Commissariat à l'Énergie Atomique, Paris, 1977).

⁹H. H. Behncke, P. Armbruster, F. Folkmann, S. Hagmann, and P. H. Mokler, in Ref. 8, p. 156.

¹⁰R. K. Cacak, Q. C. Kessel, and M. E. Rudd, *Phys. Rev. A* **2**, 1327 (1970).

¹¹D. Schwalm, A. Bamberger, P. G. Bizzezi, B. Povh, G. A. P. Engelbertink, J. W. Olness, and E. K. Warburton, *Nucl. Phys. A* **192**, 449 (1972), Appendix A. This analysis does not handle the second-order Doppler shift exactly except at 0° . We improved upon Schwalm's analysis by using Eqs. (A5), (A15), and (A19) to solve for $\cos\theta$ exactly.

¹²D. Burch, L. Wilets, and W. E. Meyerhof, *Phys. Rev. A* **9**, 1007 (1974).

¹³G. Soff, Ph.D. thesis (Universität zu Frankfurt am Main, 1976) (unpublished), p. 48.